Journal of Cardiovascular Computed Tomography 13 (2019) 86–91

Contents lists available at ScienceDirect

Journal of Cardiovascular Computed Tomography

journal homepage: www.elsevier.com/locate/jcct

Research paper

# Quantified dual energy computed tomography perfusion imaging using myocardial iodine concentration: Validation using CT derived myocardial blood flow and invasive fractional flow reserve in a porcine model

Rohan Poulter[a,*,1], David A. Wood[a], Andrew Starovoytov[a], Stephanie Smith[b], Mehran Chitsaz[c], John Mayo[a,c]

[a] Division of Cardiology, Vancouver General Hospital, 2775 Laurel Street, Vancouver, BC, V5Z 1M9, Canada
[b] Jack Bell Research Centre, Vancouver General Hospital, 2775 Laurel Street, Vancouver, BC, V5Z 1M9, Canada
[c] Department of Radiology, Vancouver General Hospital, 2775 Laurel Street, Vancouver, BC, V5Z 1M9, Canada

A B S T R A C T

*Background:* Myocardial CT perfusion imaging with dual energy (DE-CTP) can produce myocardial iodine perfusion maps. This study evaluated the accuracy of first pass myocardial iodine concentration in DE-CTP compared to CT derived dynamic myocardial blood flow (MBF) to determine regional myocardial ischemia in an animal model of coronary stenosis using invasive Fractional Flow Reserve (FFR).

*Methods:* Seven anaesthetised pigs (mean weight 51 ± 4 kg) had a graded coronary artery stenosis produced in six vessels (plus one control animal) using a methacrylate plug with FFR recorded in the target artery (ischemia = FFR < 0.80). During adenosine vasodilation, dynamic myocardial CTP and DE-CTP imaging was performed. Using vendor supplied applications, matching regions of interest (ROIs) were drawn in myocardial segments supplied by the target coronary artery to compare the two techniques.

*Results:* FFR correlated strongly to MBF (r = 0.81) and modestly to myocardial iodine concentration (r = 0.65) and myocardial CT attenuation (r = 0.62) (p < 0.0001 each). The correlation to FFR was stronger using relative ratios (absolute value/reference value of normal segments) than absolute values for MBF (r = 0.86), myocardial iodine concentration (r = 0.80) and CT number (r = 0.79) (p < 0.0001 each). Comparing normal and ischaemic territories there were significant differences in MBF (96 ± 14 vs. 27 ± 18 ml/100 ml of tissue/min, p < 0.0001), myocardial iodine concentration (3.5 ± 1 vs. 1.0 ± 0.7 mg/ml, p < 0.0001) and myocardial CT number (89 ± 9 vs. 73 ± 14 HU, p = 0.002). Myocardial iodine concentration had 91% sensitivity and 98% specificity for detecting FFR < 0.8.

*Conclusion:* Quantified myocardial iodine content from first pass DE-CTP correlates with CT derived myocardial blood flow and FFR and accurately discriminates ischemic territories in a porcine model. The accuracy and utility of myocardial iodine content in DE-CTP warrants further investigation in a clinical population with FFR as a reference standard.

## 1. Introduction

Cardiac computed tomography (CT) imaging is a well-accepted modality for the investigation of coronary artery disease[1–3] but the reporting of a high grade stenosis is not a reliable predictor of ischemia.[4–6] Techniques to evaluate myocardial CT perfusion and the ischaemic potential of atherosclerotic lesions detected on CT are therefore desirable[5,7] and multiple approaches have been developed.

Dynamic myocardial CT perfusion (CTP) imaging[8,9] tracks the transit of intravenous contrast through the myocardium to calculate regional myocardial blood flow (MBF). This demonstrates good correlation to absolute MBF in animal models[10–12] and qualitatively demonstrates defects that correlate well to single-photon emission computed tomography (SPECT) imaging.[13] In clinical studies the absolute and relative (normal versus stenosed territory) MBF can detect anatomically significant coronary artery disease,[14,15] with relative MBF better at detecting haemodynamically significant lesions.[16] The dynamic CTP technique however has higher radiation exposure and limited myocardial coverage on the z-axis[13,17] and therefore limited clinical uptake.

First pass myocardial CTP imaging applies standard cardiac CT protocols to studies performed with adenosine stress and has been shown to qualitatively identify perfusion defects in the myocardium. These correlate with defects seen on SPECT imaging[18] and add incremental value to the detection of obstructive coronary disease.[19,20]

Dual energy CT (DECT) can extend beyond CT numbers and utilise

* Corresponding author. Department of Cardiology, Sunshine Coast University Hospital, 6 Doherty St, Birtinya, Queensland, 4575, Australia.
*E-mail address:* rohan.poulter@health.qld.gov.au (R. Poulter).
[1] Permanent address: Department of Cardiology, Sunshine Coast University Hospital, 6 Doherty St, Birtinya, Queensland, Australia, 4575.

https://doi.org/10.1016/j.jcct.2019.01.020
Received 5 July 2018; Received in revised form 13 January 2019; Accepted 28 January 2019
Available online 30 January 2019

**Abbreviations**

| | |
|---|---|
| DECT | Dual energy computed tomography |
| DE-CTP | Dual energy CT perfusion |

the different absorption characteristics of iodinated contrast at different kV levels to produce a myocardial iodine map. As the presence of iodine can only occur from blood flow within the tissue delivering the contrast agent it has the potential to be a useful surrogate marker of blood flow and, when reduced, a marker of ischemia. The contrast defects[21] seen qualitatively on DECT imaging correlate with perfusion defects seen on SPECT imaging[22–24] and also indicate the presence of coronary disease.[25]

Quantitative metrics using the CT number of the myocardium during first pass myocardial CTP have also shown incremental benefit to the accuracy of coronary CT angiography.[26,27] However, CT numbers are influenced by more than just clinical (tissue and vascular) components. The technical scan acquisition parameters[28,29] and the presence of blooming or beam hardening artefact can modify the CT number. Quantified measurement of the iodine content of the myocardium may more accurately reflect true myocardial perfusion defects[30] as the iodine maps are not affected in a similar way to CT number metrics by non-perfusion factors. To date, limited studies have compared the quantified measures of myocardial iodine content in static dual energy CT perfusion (DE-CTP) imaging against SPECT imaging.[31]

The aim of this study was to evaluate quantitative myocardial iodine concentration in first pass adenosine stress DE-CTP imaging against a reference of CT derived dynamic myocardial blood flow in coronary territories supplied by normal and stenosed coronary arteries evaluated by invasive Fractional Flow Reserve.[32]

## 2. Methods

The study protocol was approved by institutional review board and University of British Columbia animal care committee (UBC Animal Care Certificate A12-0048). A technique was developed at our institution for producing a coronary stenosis with a methacrylate plug deployed using only percutaneous coronary angiography techniques in a porcine subject. Through femoral arterial access and using fluoroscopic guidance a 7FR Judkins coronary catheter was placed selectively in the target coronary artery. An 0.018 inch Certus™ Pressure Wire (St Jude Medical, MN, USA) was inserted into the target artery and using a catheter exchange technique 3.3 – 4 mm diameter methacrylate plugs (with precision drilled lumen holes of 1–2 mm diameter) were wedged in the target artery to produce graded stenoses. A 5Fr Beacon® Tip Royal Flush® Plus High-Flow multi side hole straight catheter was inserted via the femoral vein to sit in the inferior vena cava (IVC) at a level just below the right atrium to deliver drugs and contrast centrally. FFR was recorded in the target artery after 3 min of intravenous infusion of adenosine 180 μg/kg per min (Adenoscan, Sanofi-Aventis, France).

On completion of FFR assessment the animals were transported under Propofol anaesthesia to a dual source CT scanner (Somatom Definition Flash, Siemens Healthcare, Forchheim, Germany). The adenosine infusion was recommenced for a further 3 min and cardiac CT perfusion scans were performed using the following protocols:

Dynamic CT perfusion: In this axial shuttle mode, the CT scanner rapidly alternated between 2 table positions to produce repeated imaging of the myocardium over time (anatomic coverage of 73 mm z-axis with detector width of 38 mm, and a 10% overlap between both acquisition ranges). Gantry rotation time was 285 msec, slice collimation 32 × 1.2 mm and tube voltage 100 kV. Contrast (Optivue 370, Bracco Diagnostics, Ontario Canada) was injected in a monophasic bolus of 60 ml @ 6.5 ml/s via the catheter in the supra-renal IVC. Data acquisition began with commencement of the contrast injection and lasted at least 30 s. Cranial and caudal datasets were acquired every 1.5–2 s.

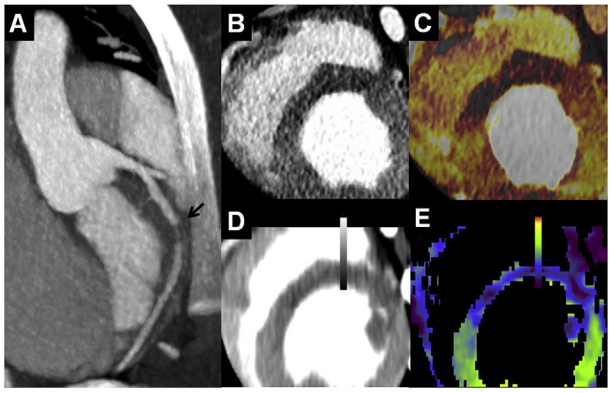


**Fig. 1.** Myocardial CT perfusion imaging of a coronary stenosis in the left anterior descending artery with FFR 0.29. The methacrylate plug is shown on MIP imaging (panel A – arrow). After first pass imaging using helical acquisition in dual energy mode a perfusion defect is visible in short axis in the anterior and antero-septal segments using CT attenuation (panel B) and in iodine overlay imaging (panel C). After dynamic shuttle mode acquisition the same perfusion defect is noted on MIP imaging (panel D) and in calculated myocardial blood flow mapping (panel E). MIP = maximum intensity projection.

First pass Dual Energy CT Perfusion: In this mode a prospective sequential acquisition was obtained using the following imaging parameters: beam collimation 64 × 0.6 mm, beam pitch 0.21, tube voltage: tube A 100 kVp, tube B 140 kVp and tube current based on subject weight (reference 370 mA). A bi-phasic contrast injection protocol [60 ml of contrast at 6.5 ml/s, followed by a 55 ml mixed saline chaser (40% contrast and 60% normal saline) was injected via the IVC catheter with real-time bolus tracking and acquisition triggered from a region of interest in the ascending aorta.

Analysis of the CT perfusion data was performed on a dedicated Siemens Multi-modality Workplace workstation. Dynamic myocardial CT perfusion data was analysed using the Volume Perfusion CT Myocardium package[12] to produce datasets of dynamic myocardial blood flow and myocardial CT number. The calculation of dynamic blood flow with this package[8,9] relies on a model of myocardial perfusion using the ratio of the maximum instantaneous slope of the myocardial tissue time attenuation curve (TAC) to the maximum value of the arterial input function (AIF), multiplied by the reciprocal of the tissue density (ρ). Dual energy CT data was analysed using the Heart Perfused Blood Volume package to derive myocardial iodine content. This is achieved using two material data points for fat and tissue and knowing the slope of the iodine enhancement vector. For each voxel of a dataset a virtual non-contrast and iodine concentration can then be produced.

For both techniques, multiple regions of interest (ROI) in each AHA myocardial segment were drawn in areas representing normal (reference) and stenosed coronary territories. The base assignment of myocardial segments to coronary territories was according to the AHA 17 segment model with modifications based on the individual coronary anatomy of each subject. The final assignment of myocardial territories to coronary arteries was determined prior to and independent of the myocardial ROI analysis. The intention was to analyse ROI in each AHA segment 1–12 with additional ROI in segment 13–16 if available. Since perfusion data were acquired from two packages the myocardial ROIs in each techniques's datasets were visually aligned for equivalent positioning in the axial slices. The CT number of the ROIs in the dynamic CT datasets were also matched with the 100 kV CT number of the dual energy dataset to aide confirmation of the visual alignment. Ischaemic segments were defined as those ROIs in territories supplied by a coronary artery whose invasive FFR measured $< 0.8$[33,34].

The relative values for MBF, myocardial iodine and CT density were

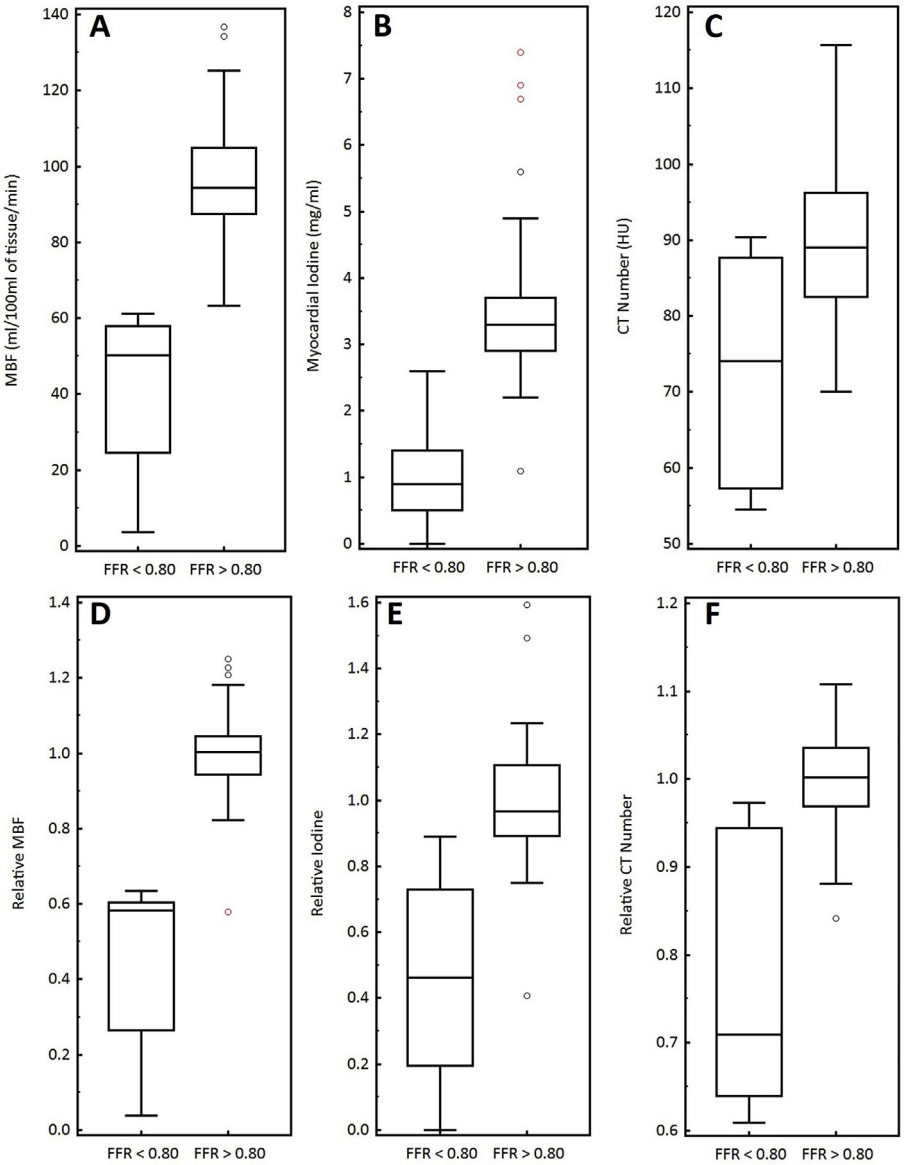


**Fig. 2.** Discrimination of CT perfusion measures in normal and ischaemic regions. Absolute values presented for (A) Dynamic CT derived myocardial blood flow) (B) Static DE-CTP derived myocardial iodine concentration (C) Myocardial CT attenuation. Relative values presented for (D) Dynamic CT derived myocardial blood flow) (E) Static DE-CTP derived myocardial iodine concentration (F) Myocardial CT attenuation.

calculated by dividing the absolute values by the average values of ROIs in segments remote to the vessel being studied (ie homogenous normal segments would have a relative value close to 1.0).

Statistical analysis of all per segment data was performed with MedCalc v11.3 (MedCalc Software; Mariakerke, Belgium). Continuous data are expressed as mean ± SD and compared using two-tailed unpaired Student *t*-test. A P value $< 0.05$ was considered significantly different. Spearman's coefficient of rank was used for correlation of techniques. Receiver operator curves (ROC) were generated for evaluating the sensitivity and specificity of each technique for detecting ischemia. The ROCs for each technique were compared using the area under the curve (AUC) in the method of DeLong.[35]

## 3. Results

Ten female Yorkshire pigs (mean weight 51 ± 4 kg) had a graded coronary artery stenosis produced and seven animals completed the study protocol (Fig. 1). Three initial subjects did not complete the protocol due to pneumothorax, thrombosis and air embolism.[36] Plugs were successfully placed in 6 subject's arteries: (2 × LAD, 2 × LCx, 2× RCA) with no plug in 1 (control). Seventy two ROI were analysed with limited myocardial coverage in the dynamic perfusion dataset precluding additional matched data points. The range of measurements were FFR 0.29–0.91, dynamic CT myocardial blood flow 3.5–136.7ml/100 ml of tissue/min, myocardial iodine concentration 0–7.4 mg/ml and myocardial CT attenuation 54–115 HU.

Comparing normal and ischaemic segments, there were significant differences in MBF (96 ± 14 vs. 27 ± 18 ml/100 ml of tissue/min, $p < 0.0001$) and myocardial iodine concentration (3.5 ± 1 vs. 1.0 ± 0.7 mg/ml, $p < 0.0001$) and myocardial CT number (89 ± 9 vs. 73 ± 14 HU, $p = 0.002$) (Fig. 2). The results were similar when the relative values were calculated: relative MBF 0.99 ± 0.1 vs. 0.31 ± 0.2 ($p = 0.0001$); relative Iodine 0.99 ± 0.2 vs. 0.28 ± 0.3 ($p = 0.0001$); relative CT number 0.99 ± 0.06 vs. 0.76 ± 0.1 ($p = 0.0001$).

FFR correlated strongly to MBF ($r = 0.81$) and modestly to myocardial iodine concentration ($r = 0.65$) and myocardial CT attenuation ($r = 0.62$) ($p < 0.0001$ each). The correlation to FFR was stronger

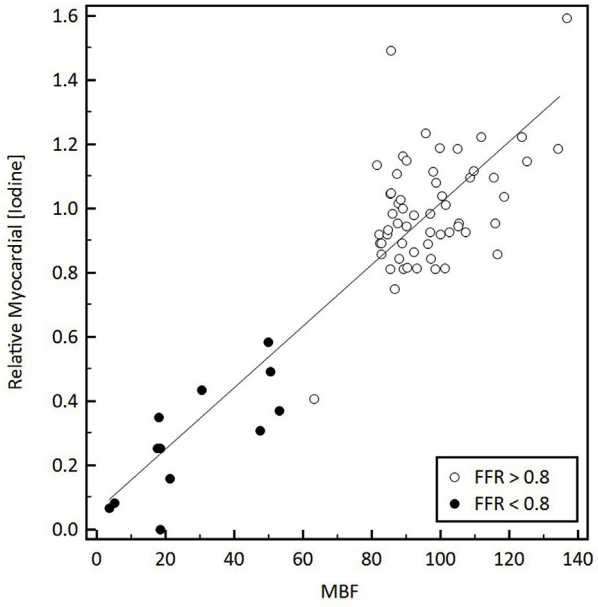


**Fig. 3.** Correlation of CT derived Myocardial Blood Flow measurement to relative myocardial iodine concentration. Subgroup indicates abnormal FFR.

using relative ratios rather than absolute values for MBF (r = 0.86), myocardial iodine concentration (r = 0.80) and CT number (r = 0.79) ($p < 0.0001$ each). The correlation between MBF and iodine concentration was modest (r = 0.42, $p < 0.0003$) but strong between MBF and relative myocardial iodine concentration (r = 0.88, $p < 0.0001$) (Fig. 3).

The performance characteristics of each CT metric to detect an FFR < 0.8 is outlined in Table 1. Comparison of the ROC curves is shown in Fig. 4. There was a significant reduction in the AUC for myocardial CT attenuation compared to myocardial blood flow and myocardial iodine concentration ($p < 0.03$). Discrimination using relative CT attenuation values was improved compared to absolute CT attenuation (AUC 0.93 vs. 0.82, p = 0.009). Relative values of MBF and myocardial iodine did not improve discrimination.

Comparing the radiation exposure from the dynamic myocardial CT perfusion and DE-CTP acquisitions showed significantly lower CTDIvol 156 ± 12 vs. 46 ± 5 ($p < 0.0001$) and DLP 1126 ± 88 vs. 630 ± 110 (p = 0.0001) for the DE-CTP study.

## 4. Discussion

This study demonstrates the assessment of myocardial iodine with DE-CTP imaging can be used as a quantified measure of myocardial perfusion to determine regions of ischemia during adenosine stress imaging. Since the model used a homogenous population of subjects with an optimised image acquisition protocol the absolute values of iodine content correlated well with FFR and had similar discrimination for ischemia as MBF. Relative MBF has previously been shown to be better than absolute MBF at discriminating ischemia and this finding was the same in our study. Relative iodine content showed a small increase in discrimination compared to absolute iodine content and correlated well with both absolute and relative myocardial blood flow. These relative values may become important when these imaging techniques are applied in a more heterogenous clinical population and subjects own normal segments can be the reference standard for determining ischaemic regions. Whilst dynamic CT derived MBF performed best at discriminating ischemia this technique has had limited clinical uptake due to radiation dose and limited scan coverage.

Quantified or semi-quantified CT metrics of myocardial perfusion based on myocardial CT number have shown utility in deriving markers for myocardial ischemia but are limited in their discriminatory ability of moderate or indeterminate lesions[26,37] by the narrow limits between normal and abnormal results.[37] This was noted in our study by the narrow differences in ratios for relative CT number between normal and ischaemic segments. In contrast the ROC curves for relative MBF and myocardial iodine showed wide differences in the values of ischaemic segments with an optimal threshold for detecting ischemia at ratios of 0.62 and 0.58 respectively. This may be due in part however to the limited sample size and extreme lower end range of FFR in the study but absolute and relative iodine content may prove to be a useful surrogate for MBF in assessing ischemia clinically.

DECT and iodine mapping overcomes some of the limitations of using CT number for CTP but DE-CTP assessment can still be affected by scan quality through cardiac motion, accuracy of data acquisition at a time of peak myocardial enhancement, and beam hardening artefacts not related to myocardial blood flow. It is unclear what impact these factors would have on quantitative DE-CTP measures and needs to be explored.

There continues to be extensive research into various CT perfusion techniques, indicating it remains unclear which method may be considered optimal. Summaries of these techniques show a similar range of diagnostic accuracy.[38–40] Dynamic CT perfusion has sensitivity 72–100%, specificity 74–100%, positive predictive value 48–100% and negative predictive value 78–100%. Single energy first pass perfusion has sensitivity 78–96%, specificity 68–98%, positive predictive value 43–96% and negative predictive value 63–98%. Qualitative assessment

**Table 1**
CT Perfusion ROC characteristics for Detecting FFR < 0.8

| | Criterion | Sens (%) | Spec (%) | PPV (%) | NPV (%) | AUC |
|---|---|---|---|---|---|---|
| MBF | 53 ml/100 ml of tissue/min | 100 | 100 | 100 | 100 | 1 |
| Myocardial [Iodine] | 1.9 mg/ml | 91 | 98 | 92 | 98 | 0.98 |
| Myocardial CT number | 76 HU | 66 | 89 | 57 | 93 | 0.82 |
| Relative MBF | 0.62 | 100 | 98 | 92 | 100 | 0.99 |
| Relative Myocardial [Iodine] | 0.58 | 100 | 98 | 92 | 100 | 0.99 |
| Relative Myocardial CT number | 0.97 | 100 | 74 | 44 | 100 | 0.93 |

ROC = Receiver Operator Curve.
FFR = fractional Flow Reserve.
Sens = sensitivity.
Spec = specificity.
PPV = positive predictive value.
NPV = negative predictive value.
AUC = Area under the curve.
MBF = Myocardial Blood Flow.

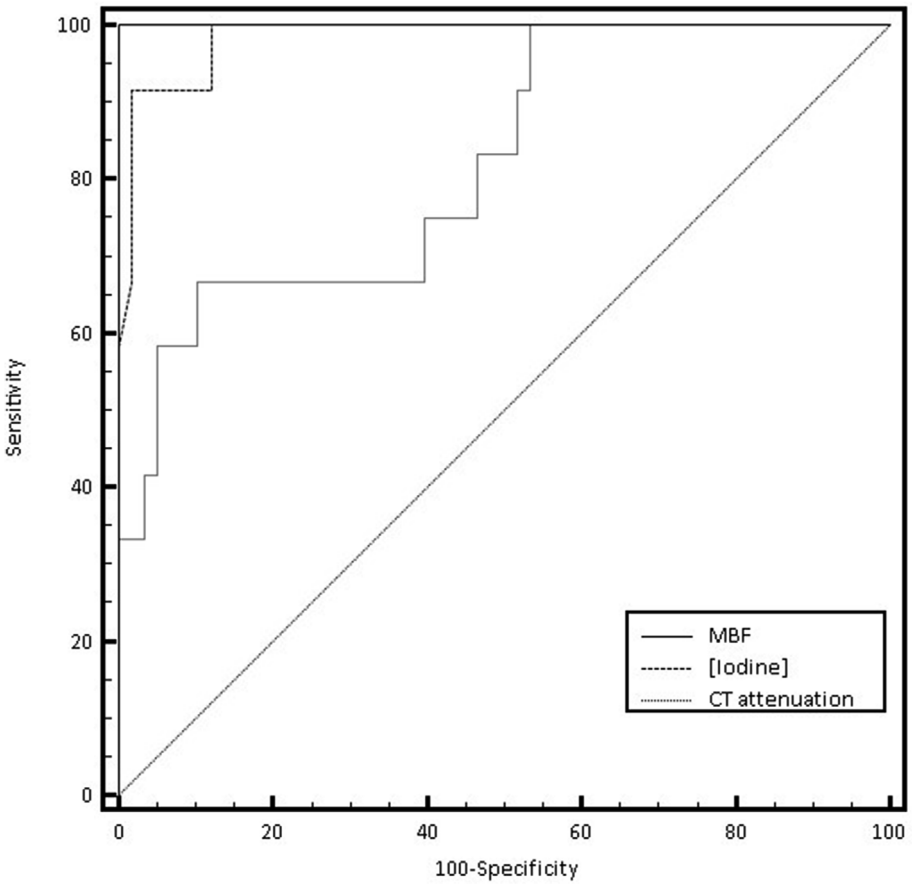


**Fig. 4.** Comparison of Receiver Operator Curves for quantified metrics of CT perfusion. The areas under the curve (AUC) are: MBF 1.0, [Iodine] 0.98, CT attenuation 0.82.
MBF = myocardial blood flow
[Iodine] = myocardial iodine content.

of DECT perfusion has a range of sensitivity 67–99%, specificity 50–99%, positive predictive value 53–92% and negative predictive value 82–98%. The current study has results within these ranges with the benefit of maintaining both excellent sensitivity and specificity.

This study is limited in the lack of a gold standard for assessment of myocardial blood flow from microspheres, MRI or PET[41,42] but the MBF derived in this study is similar to that found in earlier studies.[12,16] The excellent discrimination of normal and ischaemic segments was encouraging but may have been strengthened by the contrast injections performed centrally. With injection at the level of the right atrium there is limited opportunity for mixing and a rapid arrival of a concentrated bolus to the myocardium would improve the discrimination of both dynamic and first pass perfusion measures. The study also has limited sample size, particularly in the range of FFR values close to the 0.8 threshold. It will be crucial for the clinical utility of these methods in characterising intermediate lesions to correctly discriminate ischaemic changes close to the FFR threshold. Whilst radiation exposure was shown to be lower using the DE-CTP protocol the exposure was higher than may be needed in a clinical protocol as the study protocol did not include tube current modulation.

Finally, it's acknowledged that this technique requires a dedicated study performed with vasodilator stress when alternate techniques using analysis of resting cardiac CT datasets using computational flow dynamics have been developed.[43–46] Whilst these techniques have shown improved accuracy for determining significant coronary artery disease they also have limitations with less accuracy in borderline values (FFR 0.7 to 0.8), limited availability and long post-processing time and some limitation in the presence of calcium, stents and bypass grafts.[46,47] Therefore there may still be a role for CT perfusion techniques that can be performed with on-site analysis of the myocardium rather than off-site analysis of the coronary vessels.

## 5. Conclusion

Myocardial iodine content derived from static DE-CTP correlates with CT derived myocardial blood flow and accurately discriminates ischemic territories in a porcine model. The accuracy and utility of myocardial iodine content warrants further investigation in a clinical population with FFR as a reference standard. This will help improve patient care by ensuring indeterminate lesions on cardiac CT are classified correctly and may reduce the need for subsequent unnecessary invasive procedures.

## Conflicts of interest

None.

## Acknowledgements

Funding: This study was funded in collaboration between the Canadian Radiological Foundation, Ottawa, Canada, the Cardiology Research Fund, Vancouver General Hospital, Vancouver, Canada, and the Department of Radiology Research Fund, Vancouver General Hospital, Vancouver, Canada.

## Appendix A. Supplementary data

Supplementary data to this article can be found online at https://doi.org/10.1016/j.jcct.2019.01.020.

## References


1. Fihn SD, Gardin JM, Abrams J, et al. 2012 ACCF/AHA/ACP/AATS/PCNA/SCAI/STS guideline for the diagnosis and management of patients with stable ischemic heart disease: a report of the American college of Cardiology foundation/American heart association task force on practice guidelines, and the American college of physicians, American association for thoracic surgery, preventive cardiovascular nurses association, society for cardiovascular angiography and interventions, and society of thoracic surgeons. *J Am Coll Cardiol.* 2012;60:e44–e164.
2. Rybicki FJ, Udelson JE, Peacock WF, et al. 2015 ACR/ACC/AHA/AATS/ACEP/ASNC/NASCI/SAEM/SCCT/SCMR/SCPC/SNMMI/STR/STS appropriate utilization of cardiovascular imaging in emergency department patients with chest pain: a joint document of the American college of Radiology appropriateness criteria committee and the American college of Cardiology appropriate use criteria task force. *J Am Coll Cardiol.* 2016;67:853–879.
3. Budoff MJ, Dowe D, Jollis JG, et al. Diagnostic performance of 64-multidetector row coronary computed tomographic angiography for evaluation of coronary artery stenosis in individuals without known coronary artery disease: results from the prospective multicenter ACCURACY (Assessment by Coronary Computed Tomographic Angiography of Individuals Undergoing Invasive Coronary Angiography) trial. *J Am Coll Cardiol.* 2008;52:1724–1732.
4. Meijboom WB, Van Mieghem CA, van Pelt N, et al. Comprehensive assessment of coronary artery stenoses: computed tomography coronary angiography versus conventional coronary angiography and correlation with fractional flow reserve in patients with stable angina. *J Am Coll Cardiol.* 2008;52:636–643.
5. van Werkhoven JM, Schuijf JD, Gaemperli O, et al. Prognostic value of multislice computed tomography and gated single-photon emission computed tomography in patients with suspected coronary artery disease. *J Am Coll Cardiol.* 2009;53:623–632.
6. Kristensen TS, Engstrom T, Kelbaek H, von der Recke P, Nielsen MB, Kofoed KF. Correlation between coronary computed tomographic angiography and fractional flow reserve. *Int J Cardiol.* 2010;144:200–205.
7. Linde JJ, Sorgaard M, Kuhl JT, et al. Prediction of clinical outcome by myocardial CT perfusion in patients with low-risk unstable angina pectoris. *Int J Cardiovasc Imag.* 2017;33:261–270.
8. Bastarrika G, Ramos-Duran L, Rosenblum MA, Kang DK, Rowe GW, Schoepf UJ. Adenosine-stress dynamic myocardial CT perfusion imaging: initial clinical experience. *Invest Radiol.* 2010;45:306–313.
9. Bastarrika G, Ramos-Duran L, Schoepf UJ, et al. Adenosine-stress dynamic myocardial volume perfusion imaging with second generation dual-source computed tomography: concepts and first experiences. *Journal of cardiovascular computed tomography.* 2010;4:127–135.
10. George RT, Jerosch-Herold M, Silva C, et al. Quantification of myocardial perfusion using dynamic 64-detector computed tomography. *Invest Radiol.* 2007;42:815–822.
11. George RT, Silva C, Cordeiro MA, et al. Multidetector computed tomography myocardial perfusion imaging during adenosine stress. *J Am Coll Cardiol.* 2006;48:153–160.
12. Mahnken AH, Klotz E, Pietsch H, et al. Quantitative whole heart stress perfusion CT imaging as noninvasive assessment of hemodynamics in coronary artery stenosis: preliminary animal experience. Invest Radiol;45:298-305.
13. Ho KT, Chua KC, Klotz E, Panknin C. Stress and rest dynamic myocardial perfusion imaging by evaluation of complete time-attenuation curves with dual-source CT. *JACC Cardiovasc Imaging.* 2010;3:811–820.
14. Wichmann JL, Meinel FG, Schoepf UJ, et al. Absolute versus relative myocardial blood flow by dynamic CT myocardial perfusion imaging in patients with anatomic coronary artery disease. *AJR Am J Roentgenol.* 2015;205:W67–W72.
15. So A, Wisenberg G, Islam A, et al. Non-invasive assessment of functionally relevant coronary artery stenoses with quantitative CT perfusion: preliminary clinical experiences. *Eur Radiol.* 2012;22:39–50.
16. Kono AK, Coenen A, Lubbers M, et al. Relative myocardial blood flow by dynamic computed tomographic perfusion imaging predicts hemodynamic significance of coronary stenosis better than absolute blood flow. *Invest Radiol.* 2014;49:801–807.
17. Fujita M, Kitagawa K, Ito T, et al. Dose reduction in dynamic CT stress myocardial perfusion imaging: comparison of 80-kV/370-mAs and 100-kV/300-mAs protocols. *Eur Radiol.* 2014;24:748–755.
18. Okada DR, Ghoshhajra BB, Blankstein R, et al. Direct comparison of rest and adenosine stress myocardial perfusion CT with rest and stress SPECT. *J Nucl Cardiol.* 2010;17:27–37.
19. Rocha-Filho JA, Blankstein R, Shturman LD, et al. Incremental value of adenosine-induced stress myocardial perfusion imaging with dual-source CT at cardiac CT angiography. *Radiology.* 2010;254:410–419.
20. Penagaluri A, Higgins AY, Vavere AL, et al. Computed tomographic perfusion improves diagnostic power of coronary computed tomographic angiography in women: analysis of the CORE320 trial (coronary artery evaluation using 320-row multidetector computed tomography angiography and myocardial perfusion) according to gender. *Circ Cardiovasc Imaging.* 2016;9.
21. Johnson TR, Krauss B, Sedlmair M, et al. Material differentiation by dual energy CT: initial experience. *Eur Radiol.* 2007;17:1510–1517.
22. Blankstein R, Shturman LD, Rogers IS, et al. Adenosine-induced stress myocardial perfusion imaging using dual-source cardiac computed tomography. *J Am Coll Cardiol.* 2009;54:1072–1084.
23. Ruzsics B, Lee H, Powers ER, Flohr TG, Costello P, Schoepf UJ. Images in cardiovascular medicine. Myocardial ischemia diagnosed by dual-energy computed tomography: correlation with single-photon emission computed tomography. *Circulation.* 2008;117:1244–1245.
24. Ruzsics B, Schwarz F, Schoepf UJ, et al. Comparison of dual-energy computed tomography of the heart with single photon emission computed tomography for assessment of coronary artery stenosis and of the myocardial blood supply. *Am J Cardiol.* 2009;104:318–326.
25. Ruzsics B, Lee H, Zwerner PL, Gebregziabher M, Costello P, Schoepf UJ. Dual-energy CT of the heart for diagnosing coronary artery stenosis and myocardial ischemia-initial experience. *Eur Radiol.* 2008;18:2414–2424.
26. Kachenoura N, Gaspar T, Lodato JA, et al. Combined assessment of coronary anatomy and myocardial perfusion using multidetector computed tomography for the evaluation of coronary artery disease. *Am J Cardiol.* 2009;103:1487–1494.
27. So A, Lee TY. Quantitative myocardial CT perfusion: a pictorial review and the current state of technology development. *Journal of cardiovascular computed tomography.* 2011;5:467–481.
28. Levi C, Gray JE, McCullough EC, Hattery RR. The unreliability of CT numbers as absolute values. *AJR Am J Roentgenol.* 1982;139:443–447.
29. Sdringola S, Johnson NP, Kirkeeide RL, Cid E, Gould KL. Impact of unexpected factors on quantitative myocardial perfusion and coronary flow reserve in young, asymptomatic volunteers. *JACC Cardiovasc Imaging.* 2011;4:402–412.
30. Kang DK, Schoepf UJ, Bastarrika G, Nance Jr JW, Abro JA, Ruzsics B. Dual-energy computed tomography for integrative imaging of coronary artery disease: principles and clinical applications. *Semin Ultrasound CT MR.* 2010;31:276–291.
31. Nakahara T, Toyama T, Jinzaki M, et al. Quantitative analysis of iodine image of dual-energy computed tomography at rest: comparison with 99mtc-tetrofosmin stress-rest single-photon emission computed tomography myocardial perfusion imaging as the reference standard. *J Thorac Imag.* 2018 Mar;33(2):97–104.
32. Pijls NH, De Bruyne B, Peels K, et al. Measurement of fractional flow reserve to assess the functional severity of coronary-artery stenoses. *N Engl J Med.* 1996;334:1703–1708.
33. Tonino PA, De Bruyne B, Pijls NH, et al. Fractional flow reserve versus angiography for guiding percutaneous coronary intervention. *N Engl J Med.* 2009;360:213–224.
34. De Bruyne B, Pijls NH, Kalesan B, et al. Fractional flow reserve-guided PCI versus medical therapy in stable coronary disease. *N Engl J Med.* 2012;367:991–1001.
35. DeLong ER, DeLong DM, Clarke-Pearson DL. Comparing the areas under two or more correlated receiver operating characteristic curves: a nonparametric approach. *Biometrics.* 1988;44:837–845.
36. Poulter R, Wood DA, Starovoytov A, Smith S, Chitsaz M, Mayo J. Development of a porcine model of coronary stenosis using fully percutaneous techniques suitable for performing cardiac computed tomography, CT-perfusion imaging and fractional flow reserve. *Heart Lung Circ.* 2018 Jul 11. https://doi.org/10.1016/j.hlc.2018.06.1050 pii: S1443-9506(18)31801-8, [Epub ahead of print].
37. George RT, Arbab-Zadeh A, Miller JM, et al. Adenosine stress 64- and 256-row detector computed tomography angiography and perfusion imaging: a pilot study evaluating the transmural extent of perfusion abnormalities to predict atherosclerosis causing myocardial ischemia. *Circ Cardiovasc Imaging.* 2009;2:174–182.
38. Ko BS, Cameron JD, Defrance T, Seneviratne SK. CT stress myocardial perfusion imaging using multidetector CT–A review. *Journal of cardiovascular computed tomography.* 2011;5:345–356.
39. Pelgrim GJ, Dorrius M, Xie X, et al. The dream of a one-stop-shop: meta-analysis on myocardial perfusion CT. *Eur J Radiol.* 2015;84:2411–2420.
40. Varga-Szemes A, Meinel FG, De Cecco CN, Fuller SR, Bayer 2nd RR, Schoepf UJ. CT myocardial perfusion imaging. *AJR Am J Roentgenol.* 2015;204:487–497.
41. Bergmann SR, Herrero P, Markham J, Weinheimer CJ, Walsh MN. Noninvasive quantitation of myocardial blood flow in human subjects with oxygen-15-labeled water and positron emission tomography. *J Am Coll Cardiol.* 1989;14:639–652.
42. Krivokapich J, Smith GT, Huang SC, et al. 13N ammonia myocardial imaging at rest and with exercise in normal volunteers. Quantification of absolute myocardial perfusion with dynamic positron emission tomography. *Circulation.* 1989;80:1328–1337.
43. Koo BK, Erglis A, Doh JH, et al. Diagnosis of ischemia-causing coronary stenoses by noninvasive fractional flow reserve computed from coronary computed tomographic angiograms. Results from the prospective multicenter DISCOVER-FLOW (Diagnosis of Ischemia-Causing Stenoses Obtained via Noninvasive Fractional Flow Reserve) study. *J Am Coll Cardiol.* 2011;58:1989–1997.
44. Min JK, Leipsic J, Pencina MJ, et al. Diagnostic accuracy of fractional flow reserve from anatomic CT angiography. *J Am Med Assoc.* 2012;308:1237–1245.
45. Norgaard BL, Leipsic J, Gaur S, et al. Diagnostic performance of noninvasive fractional flow reserve derived from coronary computed tomography angiography in suspected coronary artery disease: the NXT trial (Analysis of Coronary Blood Flow Using CT Angiography: next Steps). *J Am Coll Cardiol.* 2014;63:1145–1155.
46. Cook CM, Petraco R, Shun-Shin MJ, et al. Diagnostic accuracy of computed tomography-derived fractional flow reserve : a systematic review. *JAMA Cardiol.* 2017;2:803–810.
47. Leipsic J, Yang TH, Thompson A, et al. CT angiography (CTA) and diagnostic performance of noninvasive fractional flow reserve: results from the Determination of Fractional Flow Reserve by Anatomic CTA (DeFACTO) study. *AJR Am J Roentgenol.* 2014;202:989–994.